TP53 loss-of-function mutations reduce sensitivity of acute leukaemia to the curaxin CBL0137

MICHELLE O. FORGIONE[1,2], BARBARA J. McCLURE[1,3], ELYSE C. PAGE[1,2], DAVID T. YEUNG[1,3,4], LAURA N. EADIE[1,3] and DEBORAH L. WHITE[1-3,5,6]

[1]Cancer Program, Precision Medicine Theme, South Australian Health and Medical Research Institute (SAHMRI); Faculties of [2]Science and [3]Health and Medical Science, University of Adelaide; [4]Department of Haematology, Royal Adelaide Hospital, Adelaide, South Australia 5000; [5]Australian and New Zealand Children's Haematology/Oncology Group (ANZCHOG), Melbourne, Victoria 3168; [6]Australian Genomics Health Alliance (AGHA), The Murdoch Children's Research Institute, Melbourne, Victoria 3052, Australia

Received December 19, 2021; Accepted February 28, 2022

DOI: 10.3892/or.2022.8310

Abstract. The presence of a *TP53* mutation is a predictor of poor outcome in leukaemia, and efficacious targeted therapies for these patients are lacking. The curaxin CBL0137 has demonstrated promising antitumour activities in multiple cancers such as glioblastoma, acting through p53 activation, NF-κB inhibition and chromatin remodelling. In the present study, it was revealed using Annexin-V/7-AAD apoptosis assays that CBL0137 has efficacy across several human acute leukaemia cell lines with wild-type *TP53*, but sensitivity is reduced in *TP53*-mutated subtypes. A heterozygous *TP53* loss-of-function mutation in the *KMT2A-AFF1* human RS4;11 cell line was generated, and it was demonstrated that heterozygous *TP53* loss-of-function is sufficient to cause a significant reduction in CBL0137 sensitivity. To the best of our knowledge, this is the first evidence to suggest a clinically significant role for functional p53 in the efficacy of CBL0137 in acute leukaemia. Future CBL0137 clinical trials should include *TP53* mutation screening, to establish the clinical relevance of *TP53* mutations in CBL0137 efficacy.

Correspondence to: Professor Deborah L. White, Cancer Program, Precision Medicine Theme, South Australian Health and Medical Research Institute (SAHMRI), North Terrace, Adelaide, South Australia 5000, Australia
E-mail: deborah.white@sahmri.com

Abbreviations: ALL, acute lymphoblastic leukaemia; AML, acute myeloid leukaemia; *KMT2A*r, *KMT2A*-rearranged; EFS, event-free survival; PDX, patient-derived xenograft; B-ALL, B-cell ALL; T-ALL, T-cell ALL; *TP53*^{WT} *TP53*-wild type; *TP53*^{MUT}, *TP53*-mutated

Key words: p53, TP53, curaxin, acute leukaemia, ALL, CBL0137

Introduction

Despite recent improvements in long-term survival rates for acute lymphoblastic leukaemia (ALL) (1) and acute myeloid leukaemia (AML) (2), subgroups of patients continue to experience poor long-term outcomes. *TP53* alterations are a high-risk genomic feature present in 16% of newly diagnosed ALL (3,4) and 13% of newly diagnosed AML cases (4). The presence of a *TP53* alteration is associated with poor long-term overall survival compared with *TP53* wild-type (*TP53*^{WT}) cases in both ALL (24 months vs. not reached, P=0.001) and AML (6 vs. 26 months, P<0.001) (3). To date, no targeted therapies are currently available to treat *TP53*-mutated (*TP53*^{MUT}) acute leukaemia outside of clinical trials, and more efficacious therapeutic options are required to improve long-term outcomes.

CBL0137 is a small molecule curaxin that epigenetically modulates multiple cancer-related signalling pathways (5,6), including casein kinase 2 (CK2)-mediated activation of the *TP53*-encoded p53 protein through the Facilitates Chromatin Transcription (FACT) complex (7). CBL0137 is effective in pre-clinical ALL patient-derived xenograft (PDX) models, most notably in infant *KMT2A*-rearranged (*KMT2A*r) ALL (8,9). *KMT2A*r is present in 5-10% of newly-diagnosed acute leukaemia cases overall (10), including 70-80% of infant ALL and 35-50% of infant AML diagnoses (11), and *TP53* mutations occur in ~16% of *KMT2A*r ALL cases (4). Outcomes for *KMT2A*r leukaemia are exceptionally poor across all age groups, with five-year event-free survival (EFS) rates of 30-50% (12). Evidently, advances in treatment options are required to improve patient outcomes.

In a study by Lock *et al* (8), CBL0137 induced complete remission in a *KMT2A*r infant ALL PDX model, and partial responses were observed in several B-cell ALL (B-ALL) and T-cell ALL (T-ALL) models of unknown genomic subtype. Somers *et al* (9) similarly reported CBL0137 efficacy in infant *KMT2A*r B-ALL PDX models, with responses ranging from delayed cancer progression to maintained complete remission. These early data suggested that the role of CBL0137 deserves further exploration. For instance, the presence of

loss-of-function *TP53* alterations, a reasonably common event in *KMT2A*r B-ALL, may reasonably be expected to confer resistance. Furthermore, given its *in vitro* efficacy against *KMT2A*r B-ALL, CBL0137 is also likely to be active against other subtypes of B-ALL. In the present study, it was confirmed that CBL0137 induces leukaemic cell apoptosis in a number of cell lines with various driver alterations, including those with *KMT2A* rearrangements, with LC_{50} concentrations in the range of 166 to 676 nM. Notably, it was also demonstrated that the potency of CBL0137 is attenuated in the presence of loss of function *TP53* alterations.

Materials and methods

Cell line maintenance. U-937 (CRL-1593.2), MV4;11 (CRL-9591), Jurkat (TIB-152), THP-1 (TIB-202) and RS4;11 (CRL-1873) cell lines were purchased from the American Type Culture Collection (ATCC). RCH-ACV (ACC 548), REH (ACC 22) and NALM-19 (ACC 522) cell lines were purchased from DSMZ. All cell lines were maintained in culture at 37˚C in RPMI-1640 media (cat. no. R0883; Sigma-Aldrich; Merck) containing foetal calf serum (FCS) (AU-FBS/SF; CellSera), 5 mM L-glutamine, 50 U/ml penicillin and 50 μg/ml streptomycin. THP-1 cells were cultured in 20% FCS, and all other cell lines were cultured in 10% FCS. Cells up to 20 passages from the original stock were used for experiments.

Inhibitor storage. CBL0137 (cat. no. S0507; Selleck Chemicals) was stored long-term at 10 mM in DMSO at -80˚C and diluted in DMSO immediately prior to use.

Generation of CRISPR/Cas9 TP53 knock-out RS4;11 cell lines. Vectors FUCas9mCherry and FgH1tUTG were a gift from Professor Marco Herald (Walter and Eliza Hall Institute of Medical Research, Melbourne, Australia) (13). Two independent single guide RNA (sgRNA) targets were designed, to account for off-target effects. sgRNA target sequences were designed to generate random indel and frameshift mutations in exon 4 of *TP53*, to disrupt the p53 protein prior to the critical DNA-binding domain, where deleterious *TP53* mutations identified in human leukaemia cell lines are located (Fig. 1A). sgRNA oligonucleotides were designed with online Benchling® Software (Benchling) and purchased from Sigma-Aldrich; Merck KGaA: TP53 Oligo 1 forward, 5'-TCCCACCAGCAG CTCCTACACCGG-3' and reverse, 5'-AAACCCGGTGTA GGAGCTGCTGGT-3'; and TP53 Oligo 2 forward, 5'-TCC CCCATTGTTCAATATCGTCCG-3' and reverse, 5'AAACCG GACGATATTGAACAATGG-3'.

TP53 FgH1tUTG sgRNA vectors were generated by *Bsm*BI digestion and T4 DNA ligation, incubated overnight at 4˚C and transformed by 42˚C heat shock for 2 min in DH5a™-T1^R chemically competent *E. coli* (Thermo Fisher Scientific, Inc.), and selected based on ampicillin resistance (50 μg/ml) conferred by transformation of the FgH1tUTG plasmid. Successful ligation of inserts was confirmed by Sanger sequencing with the BigDye™ Terminator v3.1 Cycle Sequencing Kit (used according to manufacturer's protocol) and SeqStudio™ Genetic Analyser System (both from Thermo Fisher Scientific, Inc.). DNA chromatogram results were analysed using online Benchling® Software.

293T cells (CRL-3216; purchased from ATCC) were co-transfected with FUCas9mCherry (4.2 μg) or FgH1tUTG sgRNA (4.2 μg) vectors, and 2nd generation lentiviral packaging vectors pMD2.G (1.6 μg), pMDLg/pRRE (2.4 μg) and pRSV-Rev (1.1 μg) (Addgene, Inc.). Each transfection was prepared in 450 μl Opti-MEM™ Reduced Serum Media and 30 μl Lipofectamine™ 2000 transfection reagent (both from Thermo Fisher Scientific, Inc.), and incubated for 1 h at room temperature prior to application to 293T cells. Viral supernatant was harvested from 293T cultures 48 h post-transfection (MOI not quantified), and RS4;11 cells were transduced by spinfection in the presence of 4 mg/ml Polybrene® (Santa Cruz Biotechnology, Inc.) at 220 x g for 1 h at room temperature in six-well tissue culture plates. One week post-transduction, GFP and mCherry double-positive populations were sorted with a BD FACSFusion flow cytometer (BD Biosciences). Sorted populations were activated with doxycycline (1 μg/ml) for 3 days, and genomic DNA was extracted by phenol-chloroform to confirm induction of frameshift mutations by PCR amplification of TP53 exon 4 using Q5® High-Fidelity DNA Polymerase (cat. no. M0491; New England Biolabs, Inc.) and the following primers: TP53 intron 4 forward, 5'-TCCTCT GACTGCTCTTTTCACCCAT-3' and reverse, 5'-AATATT CAACTTTGGGACAGGAGTCAGAGA-3'. Thermocycling conditions were as follows: 98˚C for 1 min, followed by 33 cycles at 98˚C for 10 sec, 64˚C for 15 sec and 72˚C for 2 min, followed by 1 cycle at 72˚C for 10 min. Samples were then stored at 4˚C until they were visualised in 2% agarose gel containing 1:10,000 GelRed (Biotium, Inc.).

Sanger sequencing was utilised to identify the profile of mutations present (Fig. S1). Sanger sequencing was performed using the BigDye™ Terminator v3.1 Cycle Sequencing Kit according to manufacturer's instructions (Thermo Fisher Scientific, Inc.) and SeqStudio™ Genetic Analyser System (Thermo Fisher Scientific, Inc.). DNA chromatogram results were analysed using online Benchling® Software. RNA was harvested after 7 and 14 days in culture, to quantify *TP53* expression by quantitative reverse transcription-quantitative PCR (RT-qPCR). As a comparator, RS4;11 cells expressing Cas9 vector only were used as a *TP53*^{WT} control in all relevant experiments. RT-qPCR thermocycling conditions were as follows: 10 min at 95˚C for one cycle, followed by 40 cycles at 95˚C for 15 sec and 60˚C for 60 sec. RT-qPCR cycling reactions were performed on a QuantStudio 7 Real-Time PCR system (Thermo Fisher Scientific, Inc.).

Apoptosis detection via Annexin V/7-Aminoactinomycin D staining. Cells were seeded at $2x10^5$ cells/ml and treated for 72 h with a range of CBL0137 doses in 0.3% DMSO, and incubated in 96-well tissue culture plates at 37˚C/5% CO_2 for 72 h. Treated cells were harvested at room temperature by centrifugation at 220 x g for 5 min, washed twice in flow cytometry binding buffer (Hank's Balanced Salt Solution (cat. no. H9394; Sigma-Aldrich; Merck KGaA), 10 mM HEPES, 5 mM $CaCl_2$), and cells in each well stained with Annexin V (cat. no. 556421; BD Biosciences) and 7-Aminoactinomycin (7-AAD) (cat. no. A1310; Thermo Fisher Scientific, Inc.) according to the supplier's protocol (BD Biosciences), and incubated on ice for 30 min. Assays were analysed on a BD FACSCanto flow cytometer (BD Biosciences) and data were

A

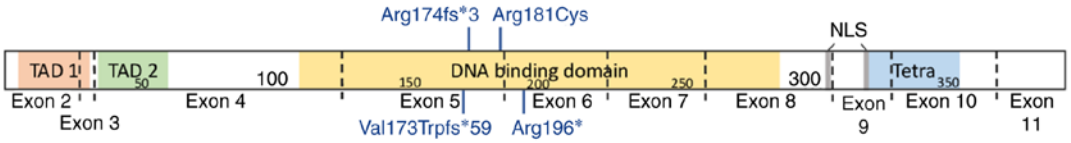

B

Cell line	*TP53* status	Cell line	*TP53* status
RS4;11, B-ALL	WT	REH, B-ALL	Heterozygous missense p.Arg181Cys
RCH-ACV, B-ALL	WT	Jurkat, T-ALL	Heterozygous p.Arg196*
NALM-19, B-ALL	WT	U-937, AMoL	Homozygous intronic splice donor site mutation resulting in p.Val173Trpfs*59 (c.599+1G>A)
MV4;11, AML	WT	THP-1, AML	Heterozygous frameshift p.Arg174fs*3

C

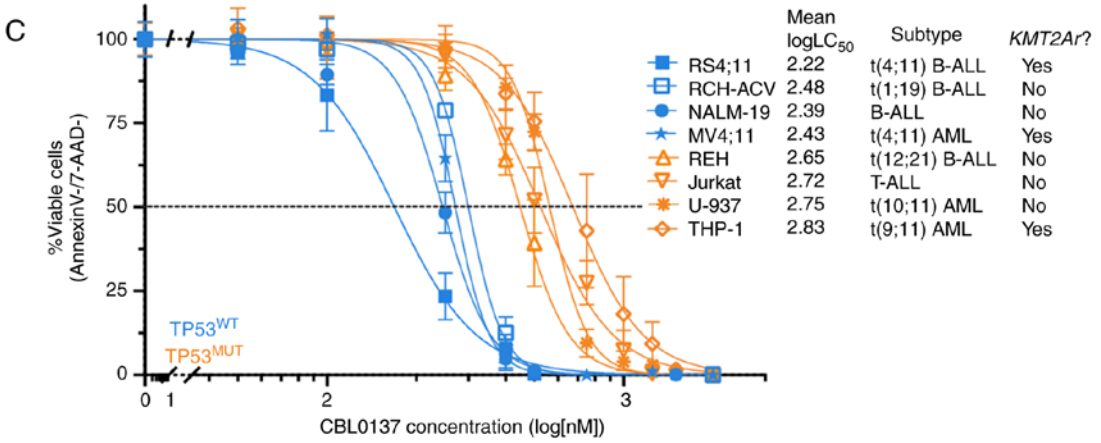

D

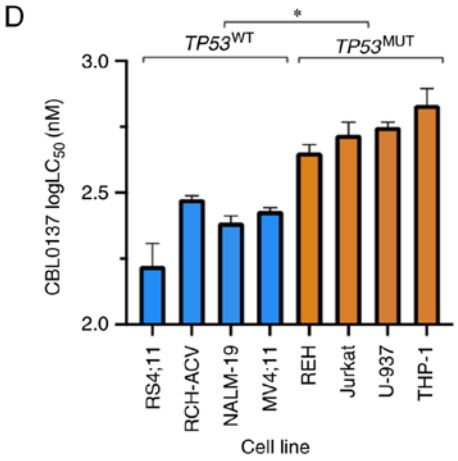

E

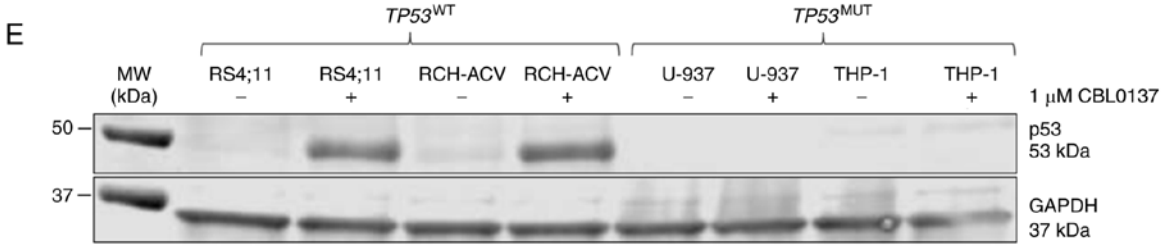

Figure 1. CBL0137 induces apoptosis in acute leukaemia cell lines, and LC_{50} are higher in *TP53*-mutated cell lines. (A) TP53 mutations identified in leukaemia cell lines. Data was obtained from the Broad Institute Cancer Cell Line Encyclopedia portal. (B) Protein domain schematic of p53, with mutations identified in cell lines annotated. Exons are denoted by dotted lines. (C) Human acute leukaemia cell lines were exposed to increasing doses of CBL0137 in duplicate and apoptosis was measured by Annexin-V/7-AAD staining after 72 h. Concentration-response curves and $logLC_{50}$ values were extrapolated using non-linear regression analysis in GraphPad Prism. Data are mean + SD for 3 biological replicates. (D) Mean CBL0137 $logLC_{50}$ values for each cell line are shown. LC_{50} values are provided in Table SII. For statistical analysis, $^{*}P<0.05$ for comparison of TP53 wild-type (TP53WT) and mutated (TP53MUT) mean $logLC_{50}$, Kruskal-Wallis test with multiple comparisons. (E) Representative immunoblot of total p53 protein in DMSO vehicle-treated (-) and 1 μM CBL0137-treated (+) cell lines. AML, acute myeloid leukaemia; AMoL, acute monocytic leukaemia; B-ALL, B-lineage acute lymphoblastic leukaemia; MUT, mutated; WT, wild-type; T-ALL, T-lineage acute lymphoblastic leukaemia; TAD, transactivation domain; NLS, nuclear localisation signal; Tetra, Tetramerisation motif.

analysed using FlowJo version 10 software (FlowJo LLC) to determine apoptotic (Annexin V and/or 7-AAD positive) and non-apoptotic (Annexin V and 7-AAD negative) populations.

The *in vitro* efficacy of CBL0137 to induce apoptosis was assessed on four *TP53*^{WT} (RS4;11, RCH-ACV, NALM-19, MV4;11) and four *TP53*^{MUT} (REH, Jurkat, U-937 and THP-1) human acute leukaemia cell lines using Annexin-V/7-AAD. The U-937 cell line was initially classified as histiocytic lymphoma (14) but is now classified as acute monocytic leukaemia (AMoL) and is therefore referred to as such throughout the manuscript (15). *TP53* mutations present in each cell line investigated are provided in Fig. 1A, obtained from the Broad Institute Cancer Cell Line Encyclopedia portal (16) (https://sites.broadinstitute.org/ccle/). All identified *TP53* mutations within the cell lines utilised are predicted to be deleterious according to COSMIC (17) (https://cancer.sanger.ac.uk) or ClinVar (18) (https://www.ncbi.nlm.nih.gov/clinvar/) databases. Later, the *in vitro* efficacy of CBL0137 to induce apoptosis was assessed on CRISPR/Cas9 *TP53* knock-out RS4;11 cell lines.

RNA analysis. RNA was extracted from $5x10^6$-$1x10^7$ cells using TRIzol® reagent (Thermo Fisher Scientific, Inc.). RNA concentration and purity were quantified with a NanoDrop 2000 Spectrophotometer (Thermo Fisher Scientific, Inc.). The QuantiTect reverse transcription kit (Qiagen GmbH) was used to synthesise cDNA from 1 μg of RNA as per manufacturer's instructions. RT-qPCR reactions were prepared in duplicate as follows: 12.5 μl RT^2 SYBR® Green ROX™ qPCR Mastermix (Qiagen GmbH), 400 nM each of forward and reverse primers, 1 μl cDNA, nuclease-free H_2O to 25 μl final volume. Cycling reactions were performed on a QuantStudio 7 Real-Time PCR system (Thermo Fisher Scientific, Inc.) with the following primers: TP53 qPCR forward, 5'-GAAGGAAATTTGCGTGTGG-3' and reverse, 5'-TGTTACACATGTAGTTGTAGTGG-3'. Values were normalised against housekeeping gene ACTB (forward, 5'-GATCATTGCTCCTCCTGAGC-3' and reverse, 5'-TCTGCGCAAGTTAGGTTTTGTC-3'). The thermocycling conditions were as aforementioned. Relative gene expression was calculated by the ΔΔCq method and fold-change expression ($2^{-\Delta\Delta Cq}$) was calculated relative to Cas9 (TP53-WT) control (19).

Protein analysis. Cells were treated for 6 h in either 0.3% DMSO or 1 μM CBL0137 (0.3% DMSO) final concentration in RPMI-1640 + 2% FCS + 50 U/ml penicillin + 50 μg/ml streptomycin. Cells were pelleted by centrifugation at 10,000 x g for 10 min at 4˚C and lysed in 60 μl 1% NP-40 (IGEPAL®) buffer (Sigma-Aldrich; Merck KGaA). Protein concentration was determined by generating a standard curve using a bicinchoninic acid (BCA) assay. Lysates were denatured and 60 μg protein was electrophoresed on 4-15% pre-cast gels (Bio-Rad Laboratories, Inc.). Proteins were transferred to polyvinylidene difluoride membranes (Bio-Rad Laboratories, Inc.) and blocked with 1X Intercept blocking buffer (LI-COR Biosciences) for 1 h at room temperature before incubation with primary antibodies (mouse anti-p53, product no. 2524; rabbit anti-p21, product no. 2947; and rabbit anti-GAPDH, product no. 2118) at 4˚C for 17-48 h. All primary antibodies were purchased from Cell Signaling Technology, Inc. and diluted at 1:1,000 in 1X Intercept blocking buffer. After washing with TBS-T (containing 0.1% Tween-20) and TBS, membranes were incubated with secondary antibodies [IRDye® 800CW anti-mouse (1:10,000) or IRDye® 800CW anti-rabbit (1:10,000)] (cat nos. 926-32212 and 925-32213, respectively; LI-COR Biosciences) for 2 h in the dark at room temperature and visualised on the LI-COR Odyssey® fluorescent scanner. For calculation of p21 expression fold change, Empiria Studio® Software version 2.0 (https://www.licor.com/bio/empiria-studio/) was used to normalise protein expression to housekeeping GAPDH protein. Fold expression change was then calculated for CBL0137-treated samples, relative to untreated samples for each respective cell line.

Statistical analysis. All calculations and statistical analysis of data were performed using GraphPad Prism Version 9.2.0 for Mac OS (GraphPad Software, Inc.). Kruskal-Wallis test with Dunn's multiple comparison post hoc test or Mann-Whitney U tests were performed to compare mean $logLC_{50}$ values between each cell line tested. $LogLC_{50}$ and LC_{50} values were extrapolated using non-linear regression analysis. All data was generated from 3 independent biological replicates. $P<0.05$ was considered to indicate a statistically significant difference.

Results

All identified *TP53* mutations within the cell lines REH, Jurkat, U-937 and THP-1 occur within a critical region of the p53 DNA binding domain (Fig. 1A and B). The presence of *TP53* loss-of-function genomic alterations significantly reduced the sensitivity of cells to CBL0137, independent of other genomic lesions present in each cell line (Fig. 1C and D). The aggregate mean $logLC_{50}$ was greater for *TP53*^{MUT} cell lines compared with *TP53*^{WT} cell lines (mean $logLC_{50}$=2.38 nM vs. 2.75 nM, P=0.046; Fig. 1D), with a more than two-fold increase in LC_{50} (Table SI). Notably, the *KMT2A* WT B-ALL cell lines NALM-19 and RCH-ACV exhibited low $logLC_{50}$ values ($logLC_{50}$=2.39 and 2.48 nM respectively; Fig. 1C). The *KMT2A*r cell line THP-1 was the most resistant cell line investigated ($logLC_{50}$=2.83 nM; Fig. 1C and D). A total of four cell lines, including two *TP53*^{WT} and two *TP53*^{MUT} were probed for the presence of total p53 protein, demonstrating increased levels of p53 following CBL0137 treatment in *TP53*^{WT} cell lines only (Fig. 1E).

To further investigate the role of p53 in CBL0137 efficacy, heterozygous *TP53* loss-of-function cell lines (*TP53*$^{+/-}$) were generated using CRISPR/Cas9 in the human *KMT2A-AFF1* ALL cell line RS4;11. The RS4;11 cell line was selected as a representative of *KMT2A*r cell lines as it is highly sensitive to CBL0137 and expresses *KMT2A-AFF1,* the most common *KMT2A*r identified in B-ALL (10). Heterozygous *TP53* loss-of-function was confirmed in cell lines by RT-qPCR and immunoblot analysis (Fig. 2A and B). Both *TP53*$^{+/-}$ cell lines exhibited a significant reduction in *TP53* expression by RT-qPCR, compared with control *TP53*^{WT} RS4;11 cells (Fig. 2A). Immunoblot analysis demonstrated that treatment with 1 μM CBL0137 stimulated p53 expression in WT RS4;11 and positive control NALM-19 cells, but this effect was abrogated in both *TP53*$^{+/-}$ RS4;11 cell lines

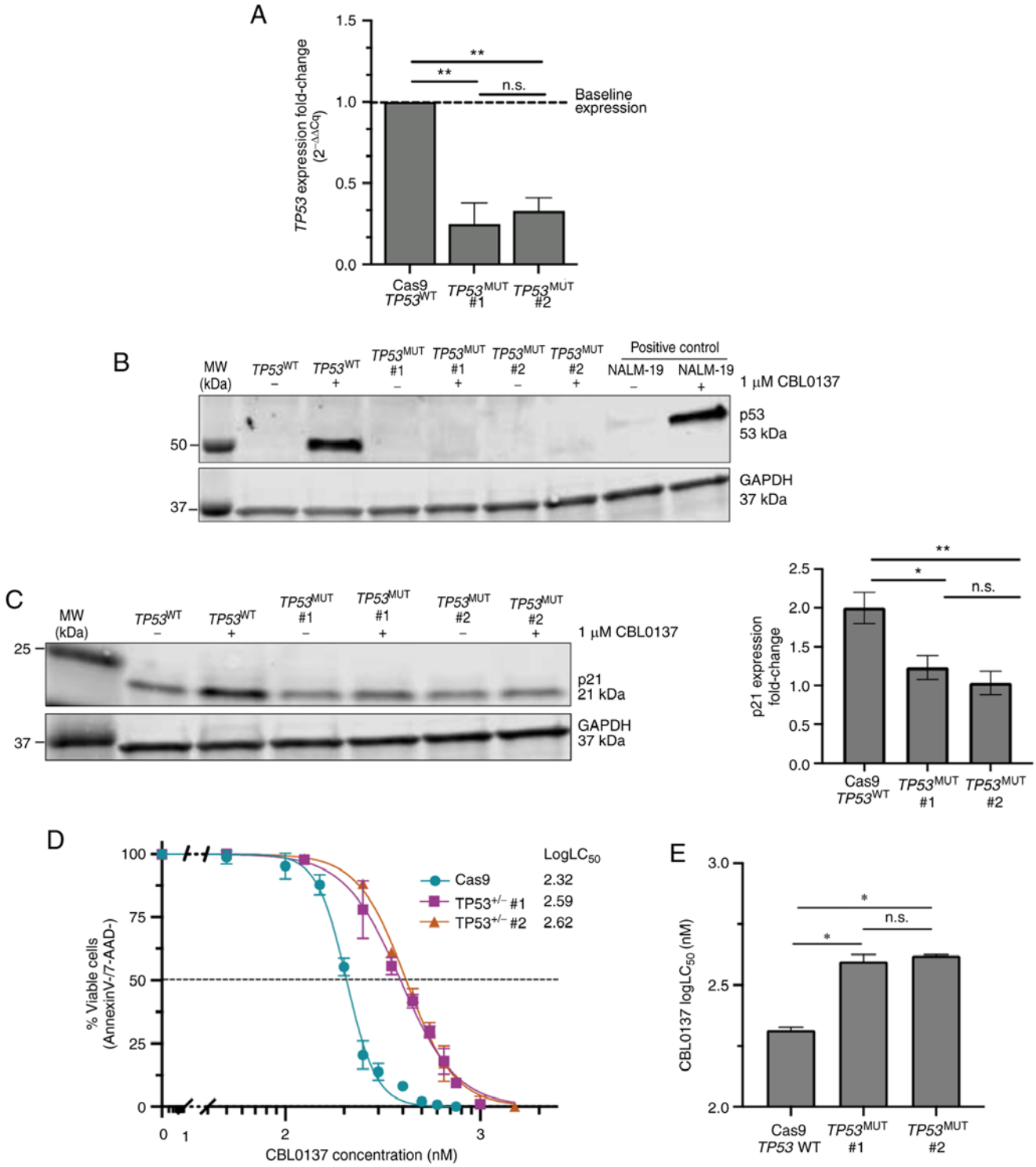

Figure 2. Heterozygous loss of *TP53* (*TP53*$^{+/-}$) promotes CBL0137 resistance in *KMT2A*r ALL. (A) Reverse transcription-quantitative PCR analysis of TP53 expression in RS4;11 cell lines validated heterozygous loss of TP53 expression. Data are mean $2^{-\Delta\Delta Cq}$ + SD, relative to Cas9 control RS4;11 cells. Baseline expression refers to TP53 expression in *TP53*^{WT} RS4;11 cells. (B) Representative immunoblot of total p53 protein in DMSO vehicle-treated (-) and 1 μM CBL0137-treated (+) RS4;11 cell lines. (C) Representative immunoblot of total p21 protein in DMSO vehicle-treated (-) and 1 μM CBL0137-treated (+) RS4;11 cell lines. Fold change in p21 expression following CBL0137 treatment was calculated relative to untreated samples, after normalizing to GAPDH. (D and E) CBL0137 dose-response and $logLC_{50}$ for *TP53*^{WT} and *TP53*^{MUT} RS4;11 cell lines, measured by Annexin-V/7-AAD apoptosis assay. LC_{50} values are provided in Table SII. Data are presented as the mean + SD. For all statistical analysis, *P<0.05 and **P<0.01, for comparison of cell lines by Kruskal-Wallis test with multiple comparisons. All data is representative of 3 independent biological replicates. *KMT2A*r, KMT2A-rearranged; ALL, acute lymphoblastic leukaemia; *TP53*^{WT} *TP53*-wild type; *TP53*^{MUT}, *TP53*-mutated; n.s., non-significant.

(Fig. 2B). The p53 effector protein p21 was upregulated ~two-fold in CBL0137-treated *TP53*^{WT} RS4;11 cells but not *TP53*^{MUT} cells, demonstrating that heterozygous *TP53* loss-of-function is sufficient to abrogate activation of downstream p53 pathways (Fig. 2C). The cell senescence effector protein p21 is a well-characterised p53 effector protein, where

p21 is rapidly activated following p53 activation, to induce cellular senescence and apoptosis (20,21). Annexin-V/7-AAD staining of $TP53^{+/-}$ cell lines revealed a ~two-fold increase in CBL0137 $\log LC_{50}$ (mean $\log LC_{50}$ WT=2.32 nM vs. $TP53^{+/-}$ #1=2.59 nM, P=0.043; WT vs. $TP53^{+/-}$ #2=2.62 nM, P=0.021; Fig. 2D and E), indicating that heterozygous *TP53* loss-of-function is sufficient to cause a significant reduction in the sensitivity of cell lines to CBL0137.

Discussion

In the present study, it was demonstrated that CBL0137 has similar potency in all tested $TP53^{WT}$ acute leukaemia cell lines, regardless of the presence of any additional genomic lesions, including *KMT2A*r. However, the presence of a *TP53* loss-of-function mutation significantly increased CBL0137 LC_{50}, with a ~2-fold increase (range 1.7-4.0-fold) compared with $TP53^{WT}$ cell lines, regardless of genotype. It was also demonstrated, for the first time to the best of our knowledge, that heterozygous *TP53* loss-of-function is alone sufficient to cause a significant increase in the LC_{50} of CBL0137 in the *KMT2A*r B-ALL cell line RS4;11.

These results suggested that CBL0137 is indeed a promising therapy which may be broadly applicable in acute leukaemia. These data also indicated that cytotoxicity of CBL0137 is not specific to *KMT2A*r, but rather the target depends on the presence or absence of functional *TP53*. Reduced sensitivity is expected in the context of *TP53* mutated malignancies, and further testing is warranted to understand the clinical significance of *TP53* mutation status in CBL0137 efficacy. It is important to note that thus far, all ALL xenograft models tested by the Pediatric Preclinical Testing Program were $TP53^{WT}$ (8). An additional 6/31 paediatric solid tumour models exhibited tumour growth delay, and 5/6 of these were $TP53^{WT}$ (8). This should also be investigated through further pre-clinical testing, and anticipated in its clinical development program. For instance, two recently completed Phase I studies of CBL0137 reported acceptable tolerability and some clinical activity against cancers of the liver, prostate, uterus, breast and ovary (22,23). The *TP53* mutational status would optimise patient selection and target those most likely to benefit from this drug for further clinical testing. It is possible that mutations in p53 downstream mediators may also influence CBL0137 potency. However, alterations within p53 downstream mediators such as *CDKN1A* (p21) and *BCL2* (BCL-2) are rarely reported in acute leukaemia. It is also possible that alterations within CK2 or the FACT complex may influence CBL0137 potency, as CBL0137-mediated activation of p53 occurs via these pathways (7), but data on the occurrence of mutations in these pathways in acute leukaemia is currently lacking (24).

The present findings highlighted the importance of p53 activation in CBL0137 efficacy in acute leukaemia, indicating that *TP53* mutation status is an important factor in the clinical application of CBL0137. There is an ongoing need to identify therapeutic strategies for patients with high-risk acute leukaemia, such as those with *TP53* mutations, to improve outcomes for these patients. The data of the present study indicated that CBL0137 is a promising anticancer therapy that depends on WT p53 activity, which thus far has not been therapeutically targetable. The clinical feasibility of CBL0137 across both $TP53^{MUT}$ and $TP53^{WT}$ malignancies will become evident as further clinical trials are performed. In the present study, it was clearly demonstrated that the potency profile of CBL0137 is tightly linked to *TP53* mutation status, and it was revealed for the first time that heterozygous *TP53* loss-of-function alone significantly affects response to CBL0137 *in vitro*. These results support the need for accurate determination of *TP53* mutation status for patients enrolling in future CBL0137 clinical trials.

Acknowledgements

The authors would like to thank Dr Randall Grose (SAHMRI, Adelaide, Australia) for his technical assistance with flow cytometric experiments.

Funding

The present study was supported in part by the National Health and Medical Research Council (NHMRC), the Bristol-Meyers Squibb company, the Tour de Cure Australia, the Leukaemia Foundation Australia and the University of Adelaide.

Availability of data and materials

The datasets used and/or analysed in the present study are available from the corresponding author on reasonable request.

Authors' contributions

MOF conceptualised the presented idea. MOF performed experiments and constructed the manuscript in consultation with BJM, ECP, DTY, LNE and DLW. MOF and BJM confirm the authenticity of all the raw data. All authors provided critical feedback and helped shape the manuscript. All authors read and approved the final manuscript.

Ethics approval and consent to participate

The present study was performed under the International Bioethics Committee (IBC) certification number BC02/2018, and all work contained within the present study was approved by the Royal Adelaide Hospital HREC committee (approval no. HREC/15/RAH/54).

Patient consent for publication

Not applicable.

Competing interests

DLW receives research support from Bristol-Meyers Squibb, and Honoraria from Bristol-Meyers Squibb and Amgen. DTY receives research support from Bristol-Meyers Squibb and Novartis, and Honoraria from Bristol-Meyers Squibb, Novartis, Pfizer and Amgen. None of these agencies have had a role in the preparation of this manuscript. All other authors declare that they have no competing interests.

References

1. Inaba H and Mullighan CG: Pediatric acute lymphoblastic leukemia. Haematologica 105: 2524-2539, 2020.
2. Shallis RM, Wang R, Davidoff A, Ma X and Zeidan AM: Epidemiology of acute myeloid leukemia: Recent progress and enduring challenges. Blood Rev 36: 70-87, 2019.
3. Stengel A, Kern W, Haferlach T, Meggendorfer M, Fasan A and Haferlach C: The impact of TP53 mutations and TP53 deletions on survival varies between AML, ALL, MDS and CLL: An analysis of 3307 cases. Leukemia 31: 705-711, 2017.
4. Stengel A, Schnittger S, Weissmann S, Kuznia S, Kern W, Kohlmann A, Haferlach T and Haferlach C: TP53 mutations occur in 15.7% of ALL and are associated with MYC-rearrangement, low hypodiploidy, and a poor prognosis. Blood 124: 251-258, 2014.
5. Kantidze OL, Luzhin AV, Nizovtseva EV, Safina A, Valieva ME, Golov AK, Velichko AK, Lyubitelev AV, Feofanov AV, Gurova KV, *et al*: The anti-cancer drugs curaxins target spatial genome organization. Nat Commun 10: 1441, 2019.
6. Dallavalle S, Mattio LM, Artali R, Musso L, Aviñó A, Fàbrega C, Eritja R, Gargallo R and Mazzini S: Exploring the interaction of curaxin CBL0137 with G-quadruplex DNA oligomers. Int J Mol Sci 22: 6476, 2021.
7. Gasparian AV, Burkhart CA, Purmal AA, Brodsky L, Pal M, Saranadasa M, Bosykh DA, Commane M, Guryanova OA, Pal S, *et al*: Curaxins: Anticancer compounds that simultaneously suppress NF-κB and activate p53 by targeting FACT. Sci Transl Med 3: 95ra74, 2011.
8. Lock R, Carol H, Maris JM, Kolb EA, Gorlick R, Reynolds CP, Kang MH, Keir ST, Wu J, Purmal A, *et al*: Initial testing (stage 1) of the curaxin CBL0137 by the pediatric preclinical testing program. Pediatr Blood Cancer 64: e26263, 2017.
9. Somers K, Kosciolek A, Bongers A, El-Ayoubi A, Karsa M, Mayoh C, Wadham C, Middlemiss S, Neznanov N, Kees UR, *et al*: Potent antileukemic activity of curaxin CBL0137 against MLL-rearranged leukemia. Int J Cancer 146: 1902-1916, 2020.
10. Forgione MO, McClure BJ, Eadie LN, Yeung DT and White DL: KMT2A rearranged acute lymphoblastic leukaemia: Unravelling the genomic complexity and heterogeneity of this high-risk disease. Cancer Lett 469: 410-418, 2020.
11. Muntean AG and Hess JL: The pathogenesis of mixed-lineage leukemia. Annu Rev Pathol 7: 283-301, 2012.
12. Marks DI, Moorman AV, Chilton L, Paietta E, Enshaie A, DeWald G, Harrison CJ, Fielding AK, Foroni L, Goldstone AH, *et al*: The clinical characteristics, therapy and outcome of 85 adults with acute lymphoblastic leukemia and t(4;11)(q21;q23)/MLL-AFF1 prospectively treated in the UKALLXII/ECOG2993 trial. Haematologica 98: 945-952, 2013.
13. Aubrey BJ, Kelly GL, Kueh AJ, Brennan MS, O'Connor L, Milla L, Wilcox S, Tai L, Strasser A and Herold MJ: An inducible lentiviral guide RNA platform enables the identification of tumor-essential genes and tumor-promoting mutations in vivo. Cell Rep 10: 1422-1432, 2015.
14. Ralph P, Moore M and Nilsson K: Lysozyme synthesis by established human and murine histiocytic lymphoma cell lines. J Exp Med 143: 1528-1533, 1976.
15. Chanput W, Peters V and Wichers H: THP-1 and U937 cells. In: The Impact of Food Bioactives on Health. Verhoeckx K, Cotter P, López-Expósito I, Kleiveland C, Lea T, Mackie A, Requena T, Swiatecka D and Wichers H (eds). Springer, Cham, pp147-159, 2015.
16. Barretina J, Caponigro G, Stransky N, Venkatesan K, Margolin AA, Kim S, Wilson CJ, Lehár J, Kryukov GV, Sonkin D, *et al*: The cancer cell line encyclopedia enables predictive modelling of anticancer drug sensitivity. Nature 483: 603-607, 2012.
17. Tate JG, Bamford S, Jubb HC, Sondka Z, Beare DM, Bindal N, Boutselakis H, Cole CG, Creatore C, Dawson E, *et al*: COSMIC: The catalogue of somatic mutations in cancer. Nucleic Acids Res 47 (D1): D941-D947, 2019.
18. Landrum MJ, Lee JM, Benson M, Brown GR, Chao C, Chitipiralla S, Gu B, Hart J, Hoffman D, Jang W, *et al*: ClinVar: Improving access to variant interpretations and supporting evidence. Nucleic Acids Res 46 (D1): D1062-D1067, 2018.
19. Zhang JD, Ruschhaupt M and Biczok R: ddCt method for qRT-PCR data analysis. Bioconductor, 2013. http://www.bioconductor.org/packages/release/bioc/vignettes/ddCt/inst/doc/rtPCR.pdf. Accessed October 26, 2021.
20. He G, Siddik ZH, Huang Z, Wang R, Koomen J, Kobayashi R, Khokhar AR and Kuang J: Induction of p21 by p53 following DNA damage inhibits both Cdk4 and Cdk2 activities. Oncogene 24: 2929-2943, 2005.
21. Xia M, Knezevic D and Vassilev LT: p21 does not protect cancer cells from apoptosis induced by nongenotoxic p53 activation. Oncogene 30: 346-355, 2011.
22. Sarantopoulos J, Mahalingam D, Sharma N, Iyer RV, Ma WW, Ahluwalia MS, Johnson S, Purmal A, Shpigotskaya P, Hards A, *et al*: Results of a completed phase I trial of CBL0137 administered intravenously (IV) to patients (Pts) with advanced solid tumors. J Clin Oncol 38 (Suppl 15): S3583, 2020.
23. Fedyanin M, Tryakin A, Lisyanskaya AS, Solovyeva E, Fadeeva N, Gladkov O, Moiseyenko V, Cheporov SV, Shpigotskaya P, Purmal A, *et al*: Results of a completed first-in-human phase Ib dose-escalation study of oral CBL0137 in patients with advanced solid tumors. J Clin Oncol 38 (Suppl 15): S3607, 2020.
24. Chua MMJ, Lee M and Dominguez I: Cancer-type dependent expression of CK2 transcripts. PLoS One 12: e0188854, 2017.